Bulgarian Journal of Veterinary Medicine, 2023, **26**, No 3, 435–454
ISSN 1311-1477; DOI: 10.15547/bjvm.2021-0048

Original article

OVARIAN AND UTERINE HAEMODYNAMICS DURING THE ESTROUS CYCLE OF EGYPTIAN BUFFALOES IN RELATION TO STEROID HORMONAL AND NITRIC OXIDE LEVELS

M. F. SAYED[1], K. H. EL-SHAHAT[1], H. EISSA[1], A. M. ABO EL-MAATY[2] & E. A. ABDELNABY[1]

[1]Theriogenology Department, Faculty of Veterinary Medicine, Cairo University, Egypt; [2]Animal Reproduction and Artificial Insemination Department, Veterinary Research Division, National Research Centre, Al Dokki, Giza, Egypt

Summary

Sayed, M. F., K. H. El-Shahat, H. Eissa, A. M. Abo El-Maaty & E. A. Abdelnaby, 2023. Ovarian and uterine haemodynamics during the estrous cycle of Egyptian buffaloes in relation to steroid hormonal and nitric oxide levels. *Bulg. J. Vet. Med.,* **26**, No 3, 435–454.

The present investigation aimed to study the ovarian and uterine haemodynamics during the estrous cycle in buffaloes in correlation with the hormonal changes (estradiol and progesterone) and nitric oxide. Six cyclic buffalo cows were scanned via transrectal Doppler ultrasonography to evaluate the normal ovarian and uterine haemodynamics through three successive estrous cycles. Results showed that the dominant follicle (F1) area, F1 diameter, area, antrum area, coloured area (pixels) and colour area % attained the highest values ($P<0.0001$) during the follicular phase. The vascularisation of F1 tended to be higher ($P>0.05$) on the day of ovulation (Day 0). The diameter and the vascularisation of the corpus luteum (CL) reached peak values ($P<0.0001$) at Day 14 and decreased to minimum values at Day 21. Plasma progesterone (P4) concentrations correlated positively with the diameter of CL ($r \leq 0.37$; $P \leq 0.01$), CL area ($r \leq 0.35$; $P \leq 0.009$), and CL colour area (pixels) ($r \leq 0.39$; $P \leq 0.001$). Besides, the estradiol (E2) level correlated with F1 diameter ($r \leq 0.19$; $P \leq 0.0001$) and F1 area ($r \leq 0.18$; $P \leq 0.0001$). Peak systolic velocity (PSV) of the ipsilateral ovarian ($P \leq 0.082$) and uterine ($P \leq 0.024$) arteries were higher than those obtained for the contralateral ones. A similar finding was obtained in end-diastolic velocity (EDV) of the ovarian arteries ($P \leq 0.005$). In conclusion, the blood flow of the ovary and uterus recorded in buffaloes varied according to the ovulating ovary, day and phase of the estrous cycle as well as with the hormonal changes.

Key words: buffaloes, follicular and luteal blood flow, ovarian, steroid hormones, uterine blood flow

INTRODUCTION

Egyptian buffalo husbandry has been conceded for centuries with widespread reproductive management systems, as this species is characterised by an increased milk fat production that involved substantial attention (Ghoneim *et al.*, 2018). In addition, buffaloes are considered the main source of meat in Egypt and many

developing countries (FAO, 2001). Buffaloes are considered poor breeders due to their low fertility (Barile, 2005; Perera, 2011). That is expressed by the delayed sexual maturity, absence of estrous expression signs, and the long postpartum anestrus. The estrous cycle duration in buffalo is very similar to that of cows with a mean duration of 21 days (Jainudeen & Hafez, 1993), but the changeability of the cycle in buffalo is usually associated with a high incidence of abnormal length of estrous cycles linked with nutritional deficiency and abnormalities in ovarian hormones secretion (Nanda *et al.*, 2003; Perera, 2008). Despite the intensive research interest in studying the haemodynamics of the female genital tract of cattle (Viana *et al.*, 2013; Lüttgenau & Bollwein, 2014; Andelnaby *et al.*, 2018) buffaloes still possess wild behaviours, so their genital tract haemodynamics had received little research interest because of the strong straining during the rectal examinations and the higher sensitivity of the rectal wall (rectal bleeding) to every examination. The follicular vascularity correlated strongly with successful pregnancy as previously mentioned in cattle (Siddiqui *et al.*, 2009), buffaloes (Samir *et al.*, 2019) and mares (Silva *et al.*, 2006).

Doppler ultrasonography is considered a non-invasive method to determine the blood velocity within the ovarian follicle and the developed corpus luteum (CL) (Brännström *et al.*, 1998; Miyazaki *et al.*, 1998). The blood flow of the follicles and/or CL correlated with their dimensions in heifers (Siddiqui *et al.*, 2009b) and mares (Ginther *et al.*, 2007). Furthermore, the changes in the follicular haemodynamics are indicators of ovulation in heifers (Siddiqui *et al.*, 2010) and mares (Acosta *et al.*, 2004).

Nitric oxide (NO) is a free radical that has been related to the mechanism of vasodilation in both male (Gur *et al.*, 2015; Abdelnaby *et al.*, 2021a) and the female genital tract (Abdelnaby *et al.*, 2020). Likewise, NO acts as a neurotransmitter as it is produced by neurons, and is metabolised to two products called nitric oxide metabolites (NOMs) in the form of nitrate and nitrite (Abdelnaby & Abo El-Maaty, 2020). Regarding vascular perfusion, NO hinders platelet aggregation, and prevents platelet adhesion with endothelial cells thus playing a direct role in the initiation of the vasodilation process in the reproductive system as previously reported in cows (Abo El-Maaty & Abdelnaby, 2017; Abdelnaby *et al.*, 2021b).

In addition, the circulating level of plasma progesterone correlates strongly with the haemodynamics of ovarian follicles and/or CL (De Tarso *et al.*, 2017). The evaluation of CL function could be observed by Doppler ultrasound. The differentiation between the functional and the non-functional CL of similar sizes could not be detected by ordinary gray-scale ultrasonography (Viana *et al.*, 2013; Pinaffi *et al.*, 2015). In buffaloes, the uterine haemodynamics in different stages of gestation was previously reported (Hussein, 2013; Varughese *et al.*, 2013; Singh *et al.*, 2018) with exception of one report in Surti buffaloes by Gaur & Purohit (2019) who reported elevated blood flow of follicles and corpus luteum at Day 0 and 13 of the estrous cycle.

Studies of follicular and luteal haemodynamics along the estrous cycle in correlation with the hormonal levels of progesterone and estrogen are not available for buffaloes while in cows, ovulation follicular dynamics and uterine blood flow have received extensive research interest. Does the ovulation in buffaloes differ from that in cows? Does the ovarian or the uterine arteries haemodynamics vary in buffaloes during the spontaneous ovulation? Several

questions need to be answered to understand the ovarian and uterine arteries haemodynamics associating follicular and luteal haemodynamics in buffaloes. Therefore, this study aimed to evaluate the dynamics of the follicular and luteal vascularisation of the spontaneous ovulations of buffalo cows, to find out the differences in the dynamics of ipsilateral or contralateral blood velocities and volumes in ovarian and uterine arteries, and to correlate the utero-ovarian vascular perfusion with estradiol, progesterone, and nitric oxide metabolites (NOMs) as a vasodilator.

MATERIALS AND METHODS

The protocol for animal experiments was ethically approved by Animal Care and Use Committee (IACUC) of Faculty of Veterinary Medicine, Cairo University: (2018-07V).

Animals and management

This study used six multiparous buffalo cows, 4–7 years of age and body weight 470–490 kg. The range of body condition score was from 2.5 to 3 according to the scoring system by Eversole *et al.* (2000). The buffaloes were raised in the research farm of the Faculty of Veterinary Medicine, Cairo University, Egypt. The farm is located in the south part of the Nile Delta (latitude 30' 01" N; longitude 31'21" E). All animals were scanned daily and completed at least three complete estrous cycles using Doppler ultrasound to record the changes in blood flow of the ovary and uterus from August 2019 to January 2020. Buffaloes were housed under natural temperature (25 °C) and daylight (10 h night). Each animal was fed a commercial concentrate ration (16% crude protein) and clover (*Trifolium alexandrinum*) *ad libitum.* Animals underwent a routine physical examination to make a confirmation on their health and reproductive status. In addition, rectal and vaginal examinations were performed for excluding any reproductive disorders.

Before the beginning of the experiments, all animals were checked for the onset of estrus twice daily and scanned by B-mode and colour mode twice a week to confirm the ovarian rebound of animals (i. e. presence of corpus luteum).

Doppler ultrasonography

All animals were subjected to trans-rectal Doppler ultrasonographic scanning to determine the follicle growth and ovulation by monitoring the corpus luteum. The ovarian structures (Fig. 1 A-D) were monitored using Real-Time B-mode 12 MHz linear array transducer (SonoAceR3, Samsung, Medison, South Korea). Ovarian follicles were counted and classified into recruited small follicles (≤5 mm), selected medium-sized (>5 to <10 mm, Fig. 1A), and deviated dominant follicle (≥10 mm, Fig. 1B, D) according to their diameter (Abdelnaby *et al.,* 2018). For blood flow mapping, the colour flow mode (CFM) was activated and the blood flow of follicle and developing CL was recorded (Fig. 1C). All the scans were performed by the same analyser. The images and video clips of B-mode, colour, and spectral Doppler were saved until further analysis. The dominant follicle (F1) was identified when its diameter reached at least 10 mm. The disappearance of the F1 and the formation of CL at its site one to two days later was considered the time of ovulation (Day 0) as previously reported by Abo El-Maaty & Abdelnaby (2017a). The measurement of the CL diameter recorded throughout the estrous cycle included the early luteal growth phase (early-luteal, days 1 to 7); luteal static phase (mid-luteal, days 8 to 14), and luteal regression phase (late-lute-

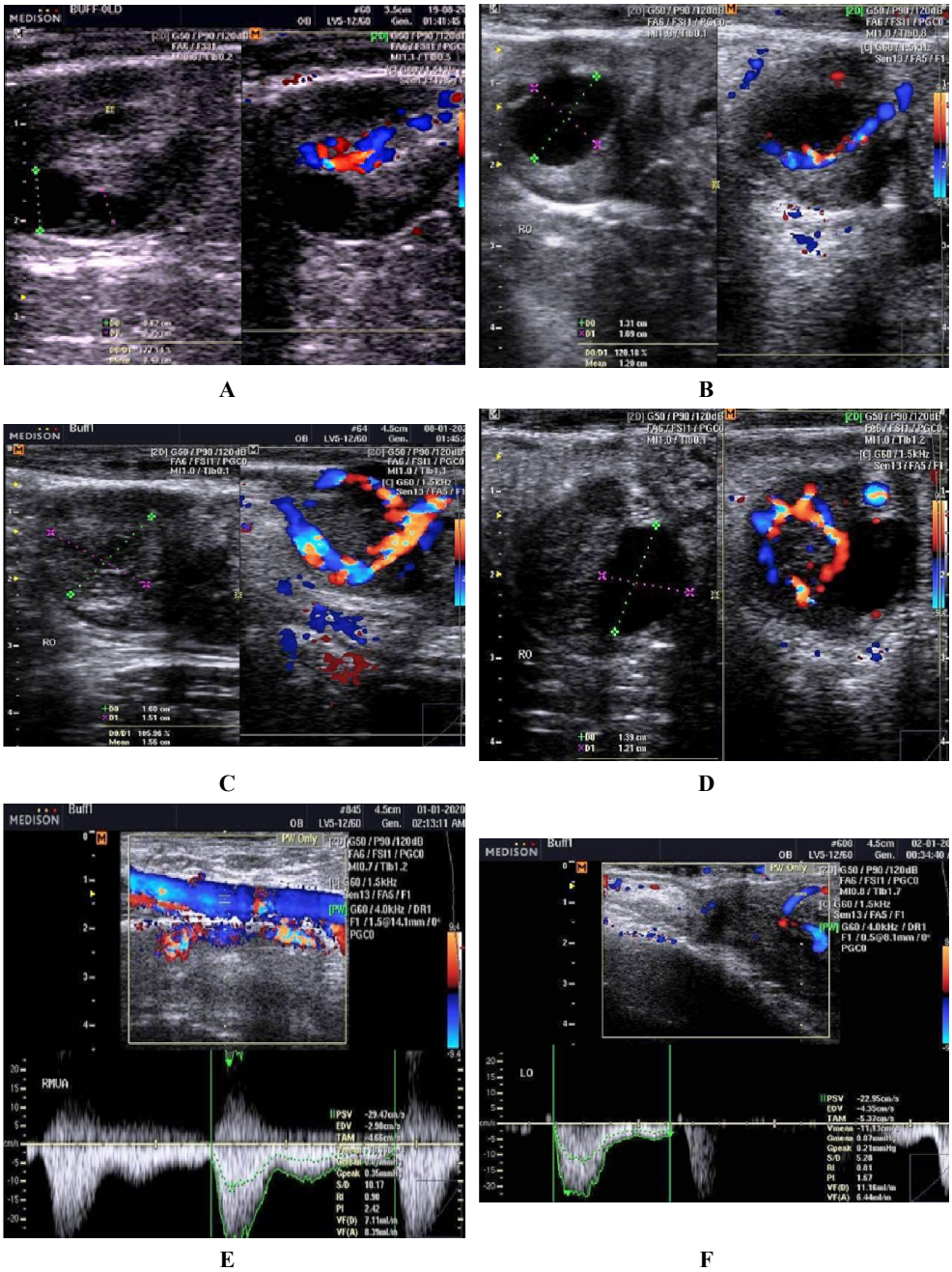

Fig. 1. Ultrasonograms revealing the ovarian follicles in grey (left split) and colour mode (right split) of the small and medium follicles on Day 6 (**A**); the large ovulating follicle (F1) on Day 0 (**B**); the mature corpus luteum on Day 7 (**C**); the regressing corpus luteum blood flow beside the next ovulating follicle on Day 13 (**D**); the middle uterine artery on Day 8 (**E**) and ovarian artery on Day 1 (**F**) with colour Doppler and their blood flow with spectral Doppler.

al, days 15 to 21; Abo El-Maaty & Abdelnaby, 2017b). Days from day –7 to ovulation (day 0) were considered the preovulatory follicular phase. The estrous phase started from the day when the dominant follicle reached 10 mm in diameter till ovulation time. The ovulation day (day 0) was the last day of the estrous phase where the last scanning of the dominant follicle indicated maximum diameter, area, antrum area, and vasculatisation area then disappeared on the following day scanning. The direction of blood flow within the uterine (Fig. 1E) and the ovarian artery (Fig. 1F) was determined by colour mode. The peak systolic velocity (PSV), end-diastolic velocity (EDV), and time-average mean velocity (TAMV) were recorded for the ipsilateral and the contralateral artery of the ovary and uterus by the spectral Doppler (Hassan *et al.,* 2017; Satheshkumar *et al.,* 2017). The resistance index (RI), the pulsatility index (PI), and the systolic/diastolic (S/D) Doppler indices were also automatically determined by the Doppler scanner. The blood flow volume (BFV) was estimated by the scanner depending on either the diameter or the area (Fig. 1E-F) of the blood vessel and those depending on the diameter (VFD) were included in the analysis. The equation of BFV = the blood vessel cross-sectional area × time-averaged velocity (TAMV) was used.

Image analysis

The stored Doppler images and video clips in the Doppler scanner were exported and analysed at each examination (Maher *et al.*, 2020a,b). The vascularisation area within the follicles and the corpora lutae of the colour Doppler mode moving toward the transducer (red) and away from the transducer (blue) were outlined using the magnetic lasso tool of the Photoshop CC software (1990–2013, Adobe Systems) to determine their areas in pixels (Abdelnaby, 2020a,b). The magnetic lasso tool was used to outline the area, the antrum area, and the coloured area then each measurement was used to count the selected areas in pixels (Abdelnaby *et al.*, 2021c). The thickness of the follicle wall (granulosa area) was estimated by measuring the area of the follicle (the external outlined boundary) then measuring the antrum area (the internal outlined one e.g. non-echogenic follicular fluid area) then the follicle wall or the granulosa area was obtained by subtracting the antrum area from the follicle area (Abdelnaby *et al.*, 2018). The percentage of the colour area in the follicle or CL was measured by dividing the colour area by their total area (Acosta *et al.,* 2003).

Blood sampling and assays

Following each Doppler ultrasound examination of buffaloes, blood samples were collected via jugular vein punctures in plain vacuum tubes. The blood samples were centrifuged at 3,000 rpm for 10 minutes and sera were harvested and stored at –20 ºC till further assay. Progesterone (P4, EIA-1561), and estradiol (E2 EIA-2693) were analysed using ELISA commercial kits (DRG, Germany). The sensitivity of the assay was 0.045 ng/mL and test intra- and inter-precisions were 5.4% and 9.96% for P4. The sensitivity of the assay for E2 was 9.7 pg/mL with test intra- and inter-precisions of 6.81% and 7.25%. The concentration of nitric oxide (NO) was measured as previously reported (Abdelnaby *et al.*, 2016; 2021d). The sensitivity of the assay was 0.225 mmol/L. The intra- assay and inter-assay coefficients of variation were 5.3% and 6.9%, respectively.

Statistical analysis

Simple one-way ANOVA was used to study the effect of days and phases of the estrous cycle of buffaloes on the follicular and luteal dynamics, haemodynamics, and the ovarian and the uterine arteries haemodynamics (SPSS 20.0, 2016). Duncan's Multiple Range Test was used to differentiate between significant means. P value <0.05 was considered significant. Phases of the estrous cycle included the luteal growth phase (days 1–7); the luteal static phase (days 8–14), and the luteal regression phases (days 15–21) whereas the period from day –7 till ovulation (day 0) was considered the pre-ovulatory phase. Paired sample t-test was used to compare the haemodynamics of the ipsilateral and the contralateral arteries of the ovarian and the uterine arteries as well as follicular and luteal parameters. Pearson correlation coefficient was used to study the correlation between blood flow parameters, ovarian hormones, and nitric oxide.

RESULTS

Follicle populations

Days of the estrous cycle of buffaloes influenced (P<0.001) the number of different follicular sizes (Table 1). The mean number of the small follicles (Fig. 2A) was high on days 10, 11, 12, and 14. However, days –7 and –5 presented a low number of small follicles that achieved a minimum on day –3 (Fig. 2A). Number of small follicles (mean ± standard deviation) on day 0 was 2.64±0.99. The number of medium follicles reached ≥2 on days –7, 2, 3, 4, 5, and 17 (Fig. 2A). Mean medium follicles number on day 0 was 1.45±0.67 while the average number of large follicles (≥ 0.50) started to increase from day –4 to reach 1.0 on day –3 then decreased again on days –2 and 0. Mean number of large follicles on day 0 was 0.73±0.45. However, days 2, 3, 5, 14, 17 had no large follicles (Fig. 2A). The mean number of the small follicles was high during the mid-luteal phase (3.25±0.83). The early luteal phase marked the highest number of medium follicles (1.97±0.77) while the follicular phase showed a high number of large follicles (0.69±0.47). During the follicular phase, mean number of total follicles reached the highest value on day 0 (4.82±0.95).

Follicle growth

The diameters of different follicular size categories were influenced (P<0.0001) by the days of the estrous cycle (Table 1). The minimum and maximum small follicles' diameters were observed on days 4 and 11 (Fig. 2B). Mean diameter of small follicles on day 0 was 4.21±0.58 mm. The diameter of the medium follicles reached 9.80 mm on day –7 which declined to low values on day –2 , day –3, and day 0 (Fig. 2B). Mean diameter of medium follicles on day 0 was 5.65±0.64 mm. The follicular phase was characterised by larger diameters of small follicles and the dominant one. The medium follicle diameter ascended linearly from the follicular phase to reach the highest value during the late luteal phase (Table 1, Fig. 2B). Three follicular growth waves could be identified in buffaloes (Fig. 2A). Wave 1 started from day –7 and ended on day 2. Wave 2 started from day 2 and ended on day 9. Wave 3 started from day 9 and ended on day 18. Depending on the increase in the number of small, medium, and large follicles (Fig. 2A) and the changes in their diameters (Fig. 2B), it could be noticed that the fate of the follicular wave ended by ovulation but the fate of the two luteal waves (waves 2,3) ended by regression or atresia.

Table 1. Effect of day and phase of estrous cycle on the follicular number, growth and haemodynamic in buffaloes (mean±SD, n=6)

Parameters	Follicular day –7 to 0	Early-luteal day 1–7	Mid-luteal day 8–14	Late-luteal day 15–21	Effect	
					Phase	day
Number of small follicles	2.51±0.91^{a}	2.97±0.73^{b}	3.25±0.83^{c}	2.71±0.46^{ab}	0.0001	0.000
Number of medium follicles	1.57±0.69^{a}	1.97±0.77^{b}	1.57±0.49^{a}	1.64±0.48^{a}	0.000	0.001
Number of large follicles	0.69±0.47^{c}	0.06±0.24^{a}	0.14±0.35^{a}	0.36±0.48^{b}	0.0001	0.000
Total number	4.77±0.80^{a}	5.00±1.01^{a}	4.96±0.78^{a}	4.79±0.57^{a}	0.169	0.077
Small diameter, mm	4.15±0.56^{b}	3.77±0.62^{a}	4.06±0.48^{b}	4.06±0.47^{b}	0.0001	0.0001
Medium diameter, mm	6.94±1.43^{a}	7.47±0.95^{b}	8.53±0.96^{c}	8.82±1.23^{c}	0.0001	0.000
F1 diameter, mm	10.82±0.75^{d}	7.47±0.95^{a}	8.73±0.84^{b}	9.66±0.57^{c}	0.0001	0.000
F1 area, px	22494±2723^{d}	12030±2818^{a}	15612±2137^{b}	18095±2255^{c}	0.0001	0.000
F1 antrum area, px	14709±1913^{d}	7180±1962^{a}	9847±182^{b}	116045±1350^{c}	0.000	0.000
F1 granulosa area, px	7785±1056^{d}	4844±949^{a}	5729±526^{b}	6490±1089^{c}	0.0001	0.000
F1 colour area, px	2087±416^{d}	598±267^{a}	997±358^{b}	1404±363^{c}	0.0001	0.0001
F1 colour, %	9.19±0.83^{d}	4.79±1.05^{a}	6.22±1.40^{b}	7.65±0.99^{c}	0.000	0.0001
Granulosa colour, %	26.69±3.27^{d}	11.96±3.52^{a}	17.10±5.13^{b}	21.41±2.66^{c}	0.0001	0.0001

Means with different superscripts (a, b, c, d) are significantly different at P<0.05, number (N), dominant follicle (F1)

Table 2. Effect of day and phase of estrous cycle on corpus luteum (CL) diameter and haemodynamics, circulating ovarian hormones estrogen (E2) and progesterone (P4), and nitric oxide (NO) in buffaloes (mean±SD, n=6)

Parameters	Follicular day –7 to 0	Early-luteal day 1–7	Mid-luteal day 8–14	Late-luteal day 15–21	Effect	
					Phase	day
CL diameter (mm)	11.39±2.37^{b}	9.72±2.38^{a}	14.40±1.17^{c}	13.81±2.18^{c}	0.000	0.000
CL area (pixel)	24960±9185^{b}	19161±8171^{a}	40292±6942^{d}	36376±10718^{c}	0.000	0.000
CL colour area (pixel)	4255±2191^{a}	4096±1949^{a}	8520±1055^{c}	6904±2271^{b}	0.000	0.000
CL colour area %	16.64±4.04^{a}	21.40±4.40^{c}	21.40±2.05^{c}	18.70±1.66^{b}	0.000	0.000
E2 (pg/mL)	109±49^{b}	95±48^{ab}	99±55^{ab}	85±45^{a}	0.041	0.563
P4 (ng/mL)	4.68±1.32^{a}	4.72±1.30^{a}	5.76±0.87^{c}	5.22±1.32^{b}	0.0001	0.0001
NO (µmol/L)	19.13±6.70^{ab}	21.03±12.04^{b}	17.67±5.18^{a}	17.80±4.66^{b}	0.031	0.002

Means with different superscripts (a, b, c, d) are significantly different at P<0.05.

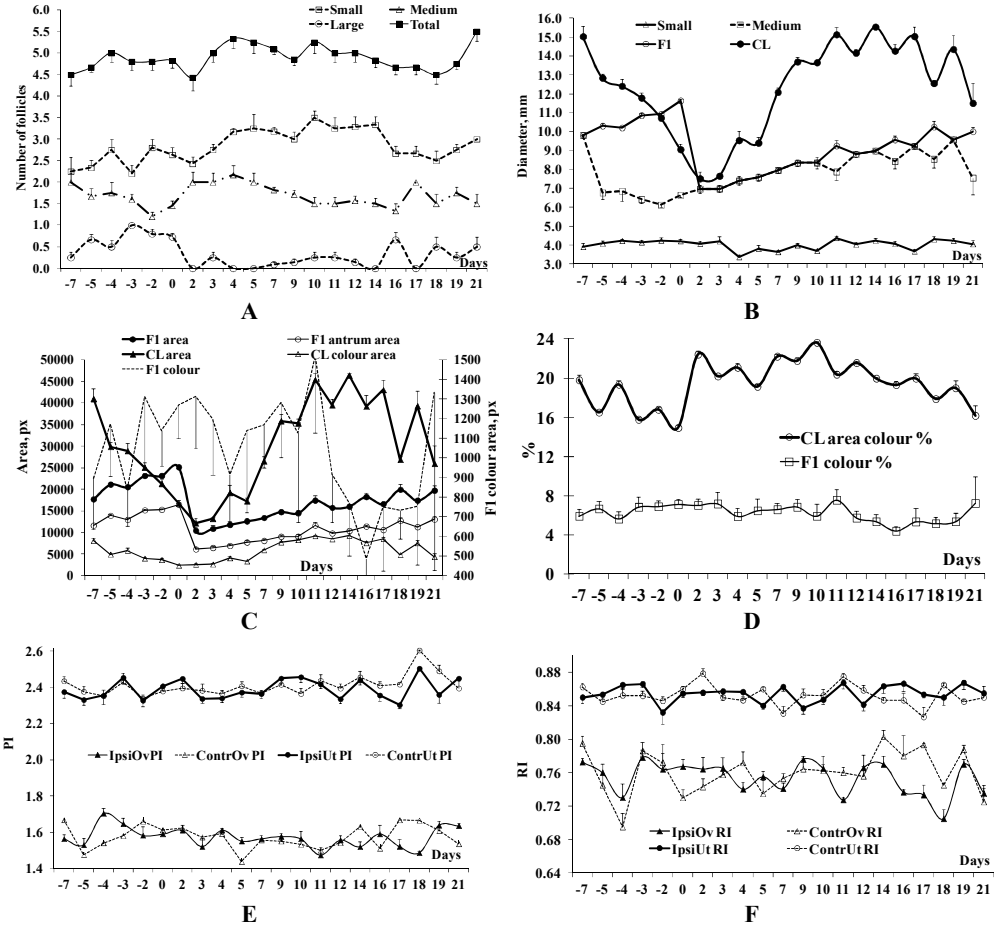

Fig. 2. A) Number of follicles; **B)** diameters of the follicles and corpus luteum (CL); **C)** dominant follicle (F1) area, F1 colour area, CL area and CL colour area; **D)** F1 and CL colour area percentages; **E)** pulsatility index (PI) of ipsilateral ovarian artery (IpsiOv), ipsilateral uterine artery (IpsiUt) contralateral ovarian artery (ContrOv) and contralateral uterine artery (ContrUt); **F)** resistance index (RI) IpsiOv, IpsiUt, ContrOv and ContrUt along the days of the estrous cycle. Data are presented as means and SD.

Corpus luteum and dominant follicle development and vascularisation

The dominant follicles (F1) started growth from day 9 then continued growth to reach a maximum mean diameter of 11.64±0.41 mm on day 0 (Fig. 2B). F1 area ascended (P≤0.0001) from day –4 to achieve a maximum value on day 0 (25137±1195 px) (Fig. 2C). F1 antrum area increased (P≤0.0001) linearly from day –4 to reach the highest value by day 0 (16446±1171 px; Fig. 2C). F1 granulosa area increased (P≤0.0001) linearly from day –5 to reach maximum value on day 0 (8691±679 px). The F1 area, antrum area, the granulose area, follicle coloured area (2512±181 px), colour area % (9.98±0.38 %), and the granulose colour area %

(29.04±2.69%) increased (P≤0.0001) linearly from the early luteal phase till their maximum values on day 0 (Table 1).

The diameter (Fig. 2B) and area (Fig. 2C) of CL increased (P≤0.0001) from day 2 till day 14 then declined to the lowest value on day 21 with a transient increase on days 17 and 19 (Table 2). The CL colour area % (Fig. 2D) had the highest values on day 10 (P≤0.0001). The lowest CL colour area (Fig. 2C) was observed on days 0 (2336±770 px) and day 2. The CL diameter, area, and colour area % (Table 2) started to increase from the early luteal phase (P≤0.0001), reached a plateau at the mid-luteal phase then decreased from the late-luteal phase to the lowest values (9.05±1.64 mm, 16712±4702 px, 14.92± 5.45%, respectively) on day 0.

When the diameter, area, colour area and colour area % of the F1 and the CL were compared using paired sample t-test (Table 3), they differed significantly (P≤0.0001). Their colour areas (r= –0.25: P≤0.0001) and the colour area % (r= –0.43: P≤0.0001) correlated negatively.

Ovarian arteries' blood flow

The PSV, EDV, and TAMV, Doppler indices (RI, PI), and BFV of both ipsilateral and contralateral ovarian arteries (Table 4) were affected by days and phases of the estrous cycle. The pulsatility index (PI) of the IpsiOv (Fig. 2E) was high (P≤0.0001) on days –3 and –4 than on days 11 and 18. The ContraOv PI increased (Fig. 2E, P≤0.0001) on day 17, day 18, day –7, and day –2 then decreased on days 5 and –5. The IpsiOv PI correlated positively with the ContraOv PI (r=0.208; P≤0.0001). The RI of the ipsilateral ovarian artery (IpsiOv, Fig. 2F) showed the lowest value on day 18 whereas the highest value (P≤0.003) was observed on day –3. RI of the contralateral ovarian artery (ContraOv, Fig. 2F) increased on day 14 compared to day –4. The IpsiOv RI correlated positively with the ContraOv RI (r=0.358; P≤0.0001). The IpsiOv RI had the lowest value (P≤0.016) during the late luteal phase compared to the follicular and the mid-luteal phases. The ContraOv RI was low (P≤ 0.016) during the follicular phase and high during the late luteal one.

The IpsiOv PSV (Fig. 3A) declined (P≤0.0001) on day 21, day 0, day –7, and day –2 and showed the lowest velocity on day –4. The ContraOv PSV (Fig. 3A) was high (P≤0.0001) on day 21, day –7, and day 3 and presented a minimum value on day 16. The IpsiOv PSV was higher (P≤0.082) than the ContraOv PSV (Table 6) and both demonstrated a week correlation (r=0.14; P≤0.011). The EDV of the IpsiOv was low (P≤0.0001; Fig. 3B) on day –4 and high on days –2, –7, and 21. The ContraOv EDV (Fig. 3B) declined (P≤0.0001) on day 16 and reached a maximum velocity on day 21. The IpsiOv EDV value was higher (P≤0.005) than those in the contralateral one with strong

Table 3. Diameter, area, colour area, and colour area percentage (mean±SD, n=6) of dominant follicle (F1) and corpus luteum (CL), and their correlation

Parameter	F1	CL	r	Correlation P value
Diameter, mm	9.15±1.57[b]	11.984±2.82[a]	0.063	0.253
Area, px	17089±4911[b]	28662±12107[a]	–0.050	0.370
Colour area, px	1282±703[b]	5644±2689[a]	–0.250	0.0001
Colour area, %	6.94±2.09[b]	19.52±4.12[a]	–0.430	0.0001

Mean with different superscripts (a, b) within the rows are significantly different at P<0.05.

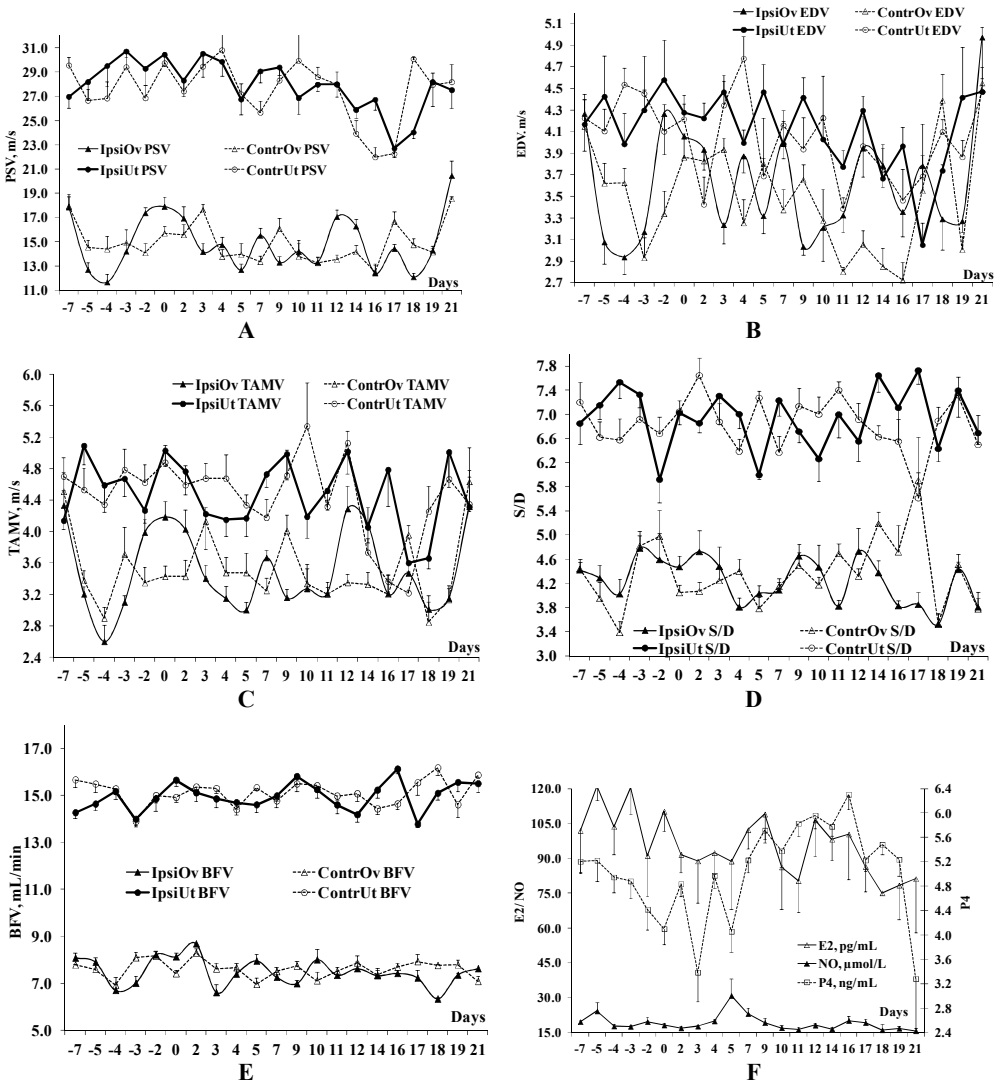

Fig. 3. A) Peak systolic velocity (PSV) of the ipsilateral ovarian and uterine arteries (IpsiOv; IpsiUt) and contralateral ovarian and uterine arteries (ContrOv; ContrUt) (**A**); **B)** end diastolic velocity (EDV) of IpsiOv, IpsiUt, ContrOv and ContrUt; **C)** time average mean velocity (TAMV) of IpsiOv, IpsiUt, ContrOv and ContrUt; **D)** systolic/diastolic velocity (S/D) of IpsiOv, IpsiUt, ContrOv and ContrUt; **E)** blood flow volume (BFV) of IpsiOv, IpsiUt, ContrOv and ContrUt; **F)** estradiol (E2); progesterone (P4) and nitric oxide (NO) concentrations concentrations during the estrous cycle of buffaloes. Data are presented as means and SD.

correlation between them (r=0.204; P≤0.0001). The ContraOv EDV reached the lowest (P≤0.003) velocity during the mid-luteal phase (Table 4). The IpsiOv TAMV (Fig. 3C) increased (P≤0.0001) on days –7, 0, 12, and day 21 and showed the lowest velocity on day –4. The ContraOv TAMV (Fig. 3C) reached a maximum

value (P≤0.0001) on day 21 and day –7 with very low velocity on day –4 and day 18. TAMV of both ovarian arteries correlated positively (r =0.127; P≤0.022). The ratio between the systolic and the diastolic velocities (S/D) of the IpsiOv (Fig. 3D) increased (P≤0.021) on day –3 compared to day 18. The ContraOv S/D (Fig. 3D) achieved a maximum (P≤0.0001; Table 4) on day 17 and a minimum on day –4. The S/D of IpsiOv and ContraOv arteries correlated positively (r=0.27; P≤0.0001). The IpsiOv S/D (P≤0.023) reached a minimum during the late luteal phase. The ContraOv S/D (P≤0.005) decreased during the follicular and the early luteal phase compared to the mid and late luteal phases.

The IpsiOv BFV (Fig. 3E) has increased (P≤0.0001; Table 4) to an optimum volume on day 2. The ContraOv BFV (Fig. 3E) achieved the highest volume (P≤0.003) on day 2 and the lowest volume on day –4 and both were strongly correlated (r=0.37; P≤0.0001). The IpsiOv BFV declined linearly (P≤0.02) from the follicular phase to reach the lowest volume during the late luteal phase (Table 4).

Uterine arteries blood flow

The IpsiUt PI increased (P≤0.0001; Fig. 2E, Table 5) to a high value on day 18 and decreased to a low value on day 17. Both uterine arteries' PI correlated positively (r=0.343; P≤0.0001; Table 6). Moreover, the maximum value of ContraUt PI was noticed (P<0001; Table 5) during the late luteal phase. RI of the ipsilateral uterine artery (IpsiUt) showed a marked increase (P≤0.001; Fig. 2F, Table 5) on days 11 and 19. The lowest value was observed on day –2. The RI of the contralateral uterine artery (ContraOv) became high on day 2 compared to day 17 (P≤0.0001; Fig. 2F). The IpsiUt PSV (Fig. 3A) increased (P≤0.004) to reach the highest velocity on day –3 and decreased gradually to the lowest one on day 17. The ContraUt PSV (Fig. 3A) increased (P≤0.0001) on day 18 and decreased to the lowest values on days 16 and 17 (Fig. 3A). The IpsiUt PSV was higher (P≤0.024) than that in the ContraUt PSV. Both IpsiUt and Contra Ut PSV correlated positively (r=0.244; P≤0.0001). The PSV of ipsilateral (P≤0.001) and contralateral (P≤0.038) uterine arteries descended linearly from the follicular phase to reach a low velocity during the late luteal phase (Table 5). The IpsiUt EDV values (Fig. 3B) were high (P≤0.04) on all days of the spontaneous ovulating estrous cycle except days 11, 14, and 18 compared to day 17 (3.05 cm/s). The ContraUt EDV was high on day –3 (4.45 cm/s), day –4 (4.54 cm/s), day 21 (4.47 cm/s), and day 4 (4.78 cm/s) compared to days 16, 2, and 11 (3.46, 3.43 and 3.39 cm/s, respectively). The correlation between EDV of the two uterine arteries was low (r=0.200; P≤0.0001). The highest ContraUt EDV (P≤0.035) was observed during the follicular phase (Table 5).

The IpsiUt TAMV (Fig. 3C) ascended (P≤0.002) on days 2, 7, 9, 12, 16, and 19 in comparison to days 17 and 18. The ContraUt TAMV (Fig. 3C) showed increments (P≤0.0001) on days 10, 12, –3, and 0 compared to days 16 and 17. The TAMV of the two uterine arteries correlated together (r =0.429; P≤0.0001; Table 6). The lowest ContraUt TAMV was obvious during the late luteal phase (Table 5). The IpsiUt S/D (Fig. 3D) increased (P≤0.001) on days 14 and 17, but decreased on days 5 and –2. The ContraUt S/D (Fig. 3D) became high (P≤0.004) on day 2 and low on day 17. The S/D of both uterine arteries correlated weekly together (r =0.112; P≤0.043).

Table 4. Effect of day and phase of estrous cycle on the ovarian arteries' haemodynamics in buffaloes (mean±SD, n=6)

Parameters	Follicular day –7 to 0	Early-luteal day 1–7	Mid-luteal day 8–14	Late-luteal day 15–21	Effect	
					Phase	day
IpsiOv RI	0.763±0.05^{b}	0.751±0.05^{ab}	0.764±0.05^{b}	0.741±0.03^{a}	0.016	0.003
ContrOv RI	0.750±0.06^{a}	0.753±0.05^{ab}	0.769±0.05^{bc}	0.772±0.05^{c}	0.015	0.0001
IpsiOv PI	1.546±0.15^{b}	1.525±0.12^{ab}	1.492±0.12^{a}	1.530±0.12^{ab}	0.042	0.001
ContrOv PI	1.539±0.15^{a}	1.515±0.12^{a}	1.506±0.14^{a}	1.547±0.11^{a}	0.210	0.0001
IpsiOv PSV	15.68±4.08^{a}	15.15±3.56^{a}	15.00±2.97^{a}	14.47±3.07^{a}	0.262	0.0001
ContrOv PSV	15.26±3.38^{a}	14.52±3.29^{a}	14.29±2.96^{a}	15.04±2.67^{a}	0.153	0.0001
IpsiOv EDV	3.69±1.19^{a}	3.78±0.78^{a}	3.49±0.93^{a}	3.65±0.81^{a}	0.254	0.0001
ContrOv EDV	3.62±0.99^{b}	3.57±0.96^{b}	3.16±0.73^{a}	3.48±0.90^{b}	0.003	0.0001
IpsiOv. TAMV	3.67±0.98^{a}	3.53±0.80^{a}	3.66±1.02^{a}	3.38±0.67^{a}	0.254	0.0001
ContrOv. TAMV	3.51±0.92^{a}	3.47±0.91^{a}	3.49±.88^{a}	3.49±0.87^{a}	0.988	0.0001
IpsiOv S/D	4.45±1.02^{b}	4.22±1.04^{ab}	4.47±1.19^{b}	3.96±0.52^{a}	0.023	0.021
ContrOv S/D	4.24±1.09^{a}	4.14±0.76^{a}	4.58±0.80^{b}	4.61±1.43^{b}	0.005	0.0001
IpsiOv BFV	77.68±10.64^{b}	75.98±11.45^{b}	74.10±11.16^{ab}	72.30±6.39^{a}	0.020	0.0001
ContrOv BFV	76.34±9.49^{a}	76.52±9.98^{a}	75.66±11.44^{a}	76.88±6.90^{a}	0.909	0.003

Ipsilateral ovarian artery (IpsiOv), contralateral ovarian artery (ContrOv), pulsatility index (PI), resistance index (RI), end-diastolic velocity (EDV), systolic/diastolic ratio (S/D), time average mean velocity (TAMV), peak systolic velocity (PSV), blood flow volume (BFV). Means with different superscripts (a, b, c) within a row are significantly different at $P<0.05$.

Table 5. Effect of day and phase of estrous cycle on the uterine arteries' haemodynamics in buffaloes (mean±SD, n=6)

Parameters	Follicular day –7 to 0	Early-luteal day 1–7	Mid-luteal day 8–14	Late-luteal day 15–21	Effect	
					Phase	day
IpsiUt RI	0.853±0.03^{ab}	0.857±0.03^{ab}	0.849±0.03^{a}	0.860±0.02^{b}	0.190	0.001
ContrUt RI	0.854±0.02^{ab}	0.850±0.04^{ab}	0.856±0.03^{b}	0.845±0.03^{a}	0.195	0.0001
IpsiUt PI	2.33±0.14^{a}	2.33±0.12^{a}	2.37±0.11^{a}	2.33±0.12^{a}	0.132	0.0001
ContrUt PI	2.33±0.12^{a}	2.33±0.11^{a}	2.37±0.13^{a}	2.41±0.11^{b}	0.001	0.001
IpsiUt PSV	29.44±5.22^{b}	28.95±5.55^{b}	27.74±3.88^{b}	26.02±4.68^{a}	0.001	0.004
ContrUt PSV	28.41±4.58^{b}	27.69±5.29^{b}	27.57±5.25^{b}	25.80±4.08^{a}	0.038	0.0001
IpsiUt EDV	4.30±1.11^{b}	4.16±0.89^{ab}	4.08±0.87^{ab}	3.94±1.05^{a}	0.177	0.040
ContrUt EDV	4.25±0.89^{b}	4.08±0.98^{ab}	3.87±1.14^{a}	3.86±1.00^{a}	0.035	0.003
IpsiUt. TAMV	4.73±1.00^{a}	4.50±1.13^{a}	4.61±1.20^{a}	4.43±1.21^{a}	0.368	0.002
ContrUt. TAMV	4.69±1.06^{b}	4.44±1.14^{b}	4.64±1.26^{b}	3.97±0.98^{a}	0.004	0.0001
IpsiUt.S/D	6.97±1.19^{a}	6.96±1.22^{a}	6.85±1.29^{a}	7.17±1.21^{a}	0.599	0.001
ContrUt.S/D	6.87±1.14^{a}	6.83±1.32^{a}	6.99±1.10^{a}	6.61±1.19^{a}	0. 417	0.004
IpsiUt BFV	149±15^{a}	149±13^{a}	150±15^{a}	152±12^{a}	0.582	0.0001
Contra Ut BFV	150±12^{a}	150±14^{a}	151±12^{a}	152±14^{a}	0.739	0.001

Ipsilateral uterine artery (IpsiUt), contralateral uterine artery (ContrUt), pulsatility index (PI), resistance index (RI), end-diastolic velocity (EDV), systolic/diastolic ratio (S/D), time average mean velocity (TAMV), peak systolic velocity (PSV), blood flow volume (BFV). Means with different superscripts (a, b) within a row are significantly different at $P<0.05$.

Table 6. Resistance index (RI), pulsatility index (PI), peak systolic velocity (PSV), end diastolic velocity (END), time average mean velocity (TAMV), systolic/diastolic ratio (S/D), blood flow volume (BFV) of the ipsilateral and the contralateral ovarian and uterine arteries (mean±SD, n=6) and their correlation

Parameter	Ipsilateral	Contralateral	r	Correlation P value
Ovarian RI	0.757±0.47	0.759±0.53	0.358	0.000
Ovarian PI	1.52±0.13	1.52±0.13	0.208	0.000
Ovarian PSV	15.19±3.55	14.77±3.174	0.140	0.011
Ovarian EDV	3.66±0.97	3.47±0.92	0.204	0.000
Ovarian TAMV	3.59±9.91	3.49±0.87	0.127	0.022
Ovarian S/D	4.32±1.03	4.35±1.004	0.270	0.000
Ovarian BVF	75.6±10.7	76.3±9.9	0.372	0.000
Uterine RI	0.85±0.03	0.85±0.03	0.031	0.573
Uterine PI	2.34±0.125	2.35±0.120	0.343	0.000
Uterine PSV	28.42±5.05	27.65±4.96	0.244	0.000
Uterine EDV	4.16±0.98	4.05±1.01	0.200	0.000
Uterine TAMV	4.59±1.120	4.52±1.145	0.429	0.000
Uterine S/D	6.96±1.23	6.86±1.19	0.112	0.043
Uterine VF(D)	149.8±14.0	150.4±12.8	0.332	0.000

The IpsiUt BFV reached peak volumes ($P \leq 0.0001$) on days 9, 16, 19, and 0 with low volumes on days –3 and 17 (Fig. 3E). The ContraUt BFV exhibited high volumes ($P \leq 0.001$) on days 18, 21, and –7 with low volume on day –3 (Fig. 3E). The BFV of the two uterine arteries correlated positively ($r=0.332$; $P \leq 0.0001$).

Blood ovarian hormones and nitric oxide levels

E2 concentrations (Fig. 3F) increased ($P<0.041$) during the follicular phase compared to the late luteal phase (Table 2). P4 concentrations decreased on day 3 and day 21 ($P \leq 0.0001$) and maintained high values from day 11 to day 16 (Fig. 3F). Blood P4 ($P \leq 0.0001$) increased linearly from the early luteal phase to reach the highest concentrations during the mid-luteal (5.76±0.87 ng/mL) then declined to reach the lowest concentrations during the follicular phase on day 0 (4.10±1.47 ng/mL). NO levels reached peak value on day 5 and descended to the lowest values during the mid-luteal phase (Table 2). P4 levels correlated with the diameter of CL ($r=0.37$; $P \leq 0.01$), CL area in pixels ($r=0.35$; $P \leq 0.009$), and CL colour area in pixels ($r=0.39$; $P \leq 0.001$).

DISCUSSION

The increase in the number of small follicles during the mid-luteal phase and that of medium follicles during the early-luteal phase in buffaloes of this study is in agreement with our previous report (El-Shahat & Kandil, 2012). The recruitment of the small follicles is continuous throughout the estrous cycle in three to four waves of growth, and the selection of the follicles during the early luteal phase is destined to regress but the selection of the follicles at the late-luteal phase is followed by deviation and ovulation which is confirmed by the growth and development of small follicles throughout the estrous cycle. A similar finding was obtained in cows (Roche *et al.*, 1991).

The ovarian follicles dynamics (recruitment and selection) was functional in

the usual manner because of the deficiency of the progesterone hormones (Roy *et al.*, 1972). The present finding demonstrated an important variation in the ovarian haemodynamics in buffaloes between the follicular and luteal phases of the estrous cycle. One of these differences is thought to be the increase in follicle area in pixels, follicle antrum area in pixels, and follicle coloured area in pixels in the follicular phase than those during the luteal one. Moreover, on the day of estrus, the blood flow in the dominant follicle achieved the highest value. Also, the percentage of coloured pixels of the dominant follicles (F1) was higher in the follicular and early luteal phases than that in the late luteal phase (6.64±2.02; 6.55±2.30 vs. 5.29±1.94, respectively). Similar finding was observed in Surti buffaloes by Gaur & Purohit (2019) where the blood flow in the largest follicle did not vary throughout the estrous cycle except near to or at the day of estrus ($P<0.05$) where this abrupt elevation in the blood flow of the ovulatory follicle was marked the time of estrus and ovulation. Similarly to our findings that the F1 area, colour area, antrum area, and granulose area increased in a linear pattern from day –7 till the highest values on the day of ovulation, in cattle, Abdelnaby *et al.* (2018) recorded that the antrum area and coloured area of ovulatory follicles increased rapidly from day –4 to reach high values on day 0. Depending on our observation, the deviation of the dominant follicle started from day 10 in a slow pattern and was completed on day 19. Once deviation is completed, the preovulatory follicle attains a larger area due to the increase of its antrum. In cattle, the blood flow of the largest follicles before deviation was similar to those in the second largest one (Acosta *et al.*, 2005).

Assessment of vasculature of CL during the estrous cycle was performed to suspect the subsequent pregnancy in Egyptian buffaloes (Lasheen *et al.*, 2018). In the present study, the size of CL and their blood flow were elevated at day 2 and reached maximum values on day 14 then decreased to reach the basal level on day 21. Similarly, the size and blood flow to CL in Surti buffaloes increased linearly from day 5 to day 13 then declined with an abrupt decrease in the CL blood flow on day 16 of the estrous cycle (Gaur & Purohit, 2019). In this study, the CL diameter decreased gradually to reach the lowest one on day 20. This decrease in CL blood flow on day 14 was attributed to the onset of luteolysis and release of PGF2a from the endometrium (Miyamoto *et al.*, 2009).

Our results showed that the PSV and EDV of the ipsilateral ovarian arteries were higher than those of the contralateral one. This was attributed to the increases in blood flow to the ovary till ovulation and after the day of ovulation (Bollwein *et al.*, 2002) while the other ovarian and uterine blood flow indices (RI, PI, TAMV, S/D, BFV) were similar during the estrous cycle. A similar finding was observed in the cow (Ando *et al.*, 2007; Abdelnaby *et al.*, 2018). The increased PSV and EDV of the ipsilateral ovarian artery could be attributed to the fact that it supplies the growing dominant follicle and the developing and mature corpus luteum and prepares the uterus to receive the ovum and maintain the conceptus if breeding is intended.

The strong association of peripheral blood progesterone with the diameter and blood flow of CL is similar to previous reports in buffaloes (Gaur & Purohit, 2019) and cows (De Tarso *et al.*, 2017). In this respect, Acosta *et al.* (2003) observed that the CL blood flow correlated

with their growth, volume, and plasma progesterone concentration. On the other hand, the levels of estrogen (E2) increased ($P<0.041$) during the follicular phase than those recorded in the late luteal phase. Also, E2 level correlated strongly with the diameter and vascularity of dominant follicles and negatively with the diameter of CL and CL area in pixels. E2 plays an essential role in the haemodynamics of the genital tract due to its vasodilator role (Acosta *et al.*, 2003). Both E2 levels and follicular blood flow increased markedly after administration of GnRH. These increased the metabolic function of the follicular cells (Acosta *et al.,* 2004). At the time of estrus, the increased E2 promoted the release of endothelial nitric oxide synthase, which abruptly increased the blood flow and vasodilatation (Acosta *et al.*, 2003). The variation of NO in buffalo serum was concomitant with the estrus phase and follicular dynamic (Abdelnaby & Abo-El-Maaty, 2020). The higher concentration of NO in the follicular phase of the estrous cycle in the present finding showed its role in follicular growth. A similar finding was obtained in mares (Abo-El-Maaty & El-Shahat, 2012). NO plays an important role in follicular development because of its many roles in vasodilatation, steroidogenesis, and control of ovarian follicular permeability (Dixit & Parvizi, 2001). The increase of blood flow to the medium follicles and their association with their highest number and the highest concentration of NO recorded during the early luteal phase of this study refer to the selection of a dominant follicle and reduced follicular atresia (Augustin *et al.*, 2001; Reynolds *et al.*, 2002).

CONCLUSION

Buffaloes showed three follicular waves. The ipsilateral ovarian and uterine arteries had higher blood flow compared to the non-ovulating contralateral ones. The corpus luteum still functioned and produced progesterone and showed vascularisation till the following ovulation time. The dominant follicle required more time from reaching 10 mm till ovulation (>7 days) and this time may depend on their blood supply through its ovarian artery. Both uterine and ovarian blood flow depended mainly on the ovulating side. The negative correlation between the CL and F1 blood flow could help in predicting the time of ovulation.

REFERENCES

Alm, H. W., H. Mlodawska, S. Torner, T. Blottner, F. B. Greising & A. Okolski, 2002. Influence of two different sera on dynamic of meiosis and extrusion of polar body during in vitro maturation of horse oocytes. *Theriogenology*, **58,** 735–738.

Abdelnaby, E. A., A. M. Abo El-Maaty, R. S. A. Ragab & A. A. Seida, 2016. Assessment of uterine vascular perfusion during the estrous cycle of mares in connection to circulating leptin and nitric oxide concentrations. *Journal of Equine Veterinary Science*, **39**, 25–32.

Abdelnaby, E. A. & A. M. Abo El-Maaty, 2017a. Dynamics of follicular blood flow, antrum growth, and angiogenic mediators in mares from deviation to ovulation. *Journal of Equine Veterinary Science*, **55**, 51–59.

Abdelnaby, E. A. & A. M. Abo El-Maaty, 2017b. Luteal blood flow and growth in correlation to circulating angiogenic hormones after spontaneous ovulation in mares. *Bulgarian Journal Veterinary Medicine*, **20**, 97–109.

Abdelnaby, E. A., A. M. Abo El-Maaty, R. S. A. Ragab & A. A. Seida, 2018. Dynamics of uterine and ovarian arteries flow velocity waveforms and their relation to follicular and luteal growth and blood flow vas-

cularization during the estrous cycle in Friesian cows. *Theriogenology*, **121,** 112–121.

Abdelnaby, E. A., 2020a. Hemodynamic changes evaluated by Doppler ultrasonographic technology in the ovaries and uterus of dairy cattle after the puerperium. *Reproductive Biology*, **20**, 202–209.

Abdelnaby, E. A., 2020b. Higher doses of melatonin affect ovarian and middle uterine arteries vascular blood flow and induce oestrus earlier in acyclic ewes. *Reproduction in Domestic Animals,* **55,** 763–769.

Abdelnaby, E. A. & A. M. Abo El-Maaty, 2020. Effect of the side of ovulation on the uterine morphometry, blood flow, progesterone, oestradiol and nitric oxide during spontaneous and induced oestrus in lactating dairy cows. *Reproduction in Domestic Animals,* **55,** 851–860.

Abdelnaby, E. A., A. M. Abo El-Maaty & D. A. El-Badry, 2020a. Ovarian and uterine arteries blood flow waveform response in the first two cycles following superstimulation in cows. *Reproduction in Domestic Animals*, **55**, 701–710.

Abdelnaby, E. A., A. M. A. El-Maaty, R. Ragab & A. Seida, 2020b. A Ovsynch produced larger follicles and corpora lutea of lower blood flow associated lower ovarian and uterine blood flows, estradiol and nitric oxide in cows. *Journal of Advanced Veterinary Research,* **10**, 165–176.

Abdelnaby, E.A., A. M. Abo El-Maaty & D. A. El-Badry, 2021a. Evaluation of ovarian hemodynamics by color and spectral Doppler in cows stimulated with three sources of follicle-stimulating hormone. *Reproductive Biology*, **21,** 100478.

Abdelnaby, E.A., I. A. Emam & A. M. Fadl, 2021b. Assessment of the accuracy of testicular dysfunction detection in male donkey (*Equus asinus*) with the aid of colour-spectral Doppler in relation to plasma testosterone and serum nitric oxide levels. *Reproduction in Domestic Animals*, doi: 10.1111/rda.13916.

Abdelnaby, E.A., Y.S. Abouelela & N.A.E. Yasin, 2021c. Evaluation of penile blood flow in dogs with tvt before and after chemotherapeutic treatment with special reference to its angioarchitecture. *Advances in Animals and Veterinary Sciences,* **9**, 1159–1168.

Abdelnaby, E. A., K. G. Abd El khalek & I. A. Emam, 2021d. The beneficial effects of enriched diet on testicular blood flow and seminal parameters using colour and pulsed Doppler ultrasound in dogs. *Bulgarian Journal of Veterinary Medicine* (online first), http://tru.uni-sz.bg/bjvm/2021-0037%20OnFirst.pdf (13 August 2021 date last accessed).

Abo-El Maaty, A. M. & K. H. El-Shahat, 2012. Hormonal and biochemical serum assay in relation to the estrous cycle and follicular growth in Arabian mare. *Asian Pacific Journal of Reproduction,* **1**, 105–110.

Abo El-Maaty, A. M. & E. A. Abdelnaby, 2017. Follicular blood flow, antrum growth and angiogenic mediators in mares from ovulation to deviation. *Animal Reproduction*, **14**, 1043–1056.

Acosta, T., K. Hayashi, M. Ohtani & A. Miyamoto, 2003. Local changes in blood flow within the pre ovulatory follicle wall and early corpus luteum in cows. *Reproduction,* **125**, 759–767.

Acosta, T. J., E. L. Gastal, M. O. Gastal, M. A. Beg & O. J. Ginther, 2004. Differential blood flow changes between the future dominant and subordinate follicles precede diameter changes during follicle selection in mares. *Biology of Reproduction*, **71**, 502–507.

Acosta, T. J., K. G. Hayashi, M. Matsui & A. Miyamoto, 2005. Changes in follicular vascularity during the first follicular wave in lactating cows. *Journal of Reproduction and Development*, **51**, 273–280.

Ando, T., S. Kamimura, K. Haman, H. Ohtsuka & D. Watanabe, 2007. Uterine and ovarian blood flow in a Holstein Friesian cow with aplasia of one uterine horn. *Journal of Veterinary Medical Science*, **69,** 429–432.

Augustin, H. G., 2001. Vascular morphogenesis in the ovary. In: *Vascular Morphogenesis in the Female Reproductive System,* Birkhauser Boston, New York, pp. 109–130.

Barile, V. L., 2005. Improving reproductive efficiency in female buffaloes. *Livestock Production Science,* **92**, 183–194.

Bollwein, H., F. Weber, B. Kolberg & R. Stolla, 2002. Uterine and ovarian blood flow during the estrous cycle in mares. *Theriogenology*, **65**, 2129–2138.

Brännström, M., U. Zackrisson, H. G. Hagström, B. Josefsson, P. Hellberg, S. Granberg & T. Bourne, 1998. Preovulatory changes of blood flow in different regions of the human follicle. *Fertility and Sterility*, **69**, 435–442.

De Tarso, S. G. S., G. D. A. Gastal, S. T. Bashir, M. O. Gastal, G. A. Apgar & E. L. Gastal, 2017. Follicle vascularity coordinates corpus luteum blood flow and progesterone production. *Reproduction Fertility Development,* **29**, 448.

Dixit, D. A & N. Parvizi, 2001. Nitric oxide and the control of reproduction. *Animal Reproduction Science*, **65**, 1–16.

El-Shahat, K. H. & M. Kandil, 2012. Antioxidant capacity of follicular fluid in relation to follicular size and stage of estrous cycle in buffaloes. *Theriogenology*, **77**, 1513–1518.

Eversole, D. E., M. F. Browne, J. B. Hall & R. E. Dietz, 2000. Body condition scoring beef cows. Blacksburg, VA Virginia Polytechnic Institute and State University. 6. Virginia Cooperative Extension Publication, 400-795.

FAO, 2001. http://www.fao.org.

Frazer, H. M., 2006. Regulation of the ovarian follicular vasculature. *Reproductive Biology and Endocrinology*, **4**, 18.

Gaur, M. & G. Purohit, 2019. Follicular dynamics and color Doppler vascularity evaluations of follicles and corpus luteum in relation to plasma progesterone during the oestrous cycle of Surti buffaloes. *Reproduction in Domestic Animals*, **54**, 585–594.

Ghoneim, E. M., S. Omar & E. El-Dahshan, 2018. Measuring welfare of egyptian buffaloes in different management systems. *Journal of Animal and Poultry Production, Mansoura University*, **9**, 407–414.

Ginther, O. J., 2007. Ultrasound Imaging and Animal Reproduction: Color-Doppler ultrasonography, ed O. J. Ginther, Cross Plains: Equi Services Publishing.

Gur, S., P. J. Kadowitz, S. C. Sikka, T. C. Peak & W. J. Hellstrom, 2015. Overview of potential molecular targets for hydrogen sulfide: A new strategy for treating erectile dysfunction. *Nitric oxide: Biology and Chemistry*, **50**, 65–78.

Hassan, M., A. Sattar, M. Bilal, M. Avais & N. Ahmad, 2017. Evaluation of changes in blood flow of the uterine artery by Doppler ultrasonography during the estrous cycle in lactating *Bos indicus* cows. *Animal Reproduction Science,* **184**, 78–85.

Hussein, H. A., 2013. Validation of color Doppler ultrasonography for evaluating the uterine blood flow and perfusion during late normal pregnancy and uterine torsion in buffaloes. *Theriogenology*, **79**, 1045–1053.

Jainudeen, M. R. & E. S. E. Hafez, 1993. Cattle and buffalo. In: *Reproduction in Farm Animals*, 6th edn, ed E. S. E. Hafez, Lea and Febiger, Philadelphia, USA, pp. 315–329.

Lasheen, M. E., H. M. Badr, M. M. Kandiel, A. M. Abo El-Maaty, H. Samir, M. Farouk & M. H. Eldawy. 2018. Predicting early pregnancy in Egyptian buffalo cows via measuring uterine and luteal blood flows, and serum and saliva progesterone. *Tropical Animal Health and Production,* **50**, 137–142.

Lüttgenau, J. & H. Bollwein, 2014. Evaluation of bovine luteal blood flow by using color Doppler ultrasonography. *Reproduction Biology,* **14**, 103–109.

Maher, M. A., H. A. M. Farghali, E. A. Abdelnaby & I. A. Emam, 2020a. Gross anatomical, radiographic and doppler sonographic approach to the infra-auricular parotid region in donkey (*Equus asinus*).

Journal of Equine Veterinary Science, **88**, 102968.

Maher, M. A., H. A. M. Farghali, A. H. Elsayed, I. A. Emam, E. A. Abdelnaby & R. T. Reem, 2020b.A potential use of doppler sonography for evaluating normal hemodynamic values of the hepatic, pancreatic and splenic vessels in domestic rabbits. *Advances in Animal and Veterinary Sciences*, **5**, 506–518.

Miyamoto, A. & K. Shirasuna, 2009. Luteolysis in the cow: A novel concept of vasoactive molecules. *Animal Reproduction,* **6**, 47–59.

Miyazaki, T., M. Tanaka, K. Miyakoshi, K. Minegishi, K. Kasai & Y. Yoshimura, 1998. Power and color Doppler ultrasonography for the evaluation of the vasculature of the human corpus luteum. *Human Reproduction,* **13**, 2836–2841.

Nanda, A. S., P. S. Brar & S. Prabhakar, 2003. Enhancing reproductive performance in dairy buffalo: Major constraints and achievements. *Reproduction*, **61** (Suppl.), 27–36.

Perera, B. M. A. O., 2008. Reproduction in domestic buffalo. *Reproduction in Domestic Animals,* **43** (Suppl.), 200–206.

Perera, B. M. A. O., 2011. Reproductive cycles of buffalo. *Animal Reproduction Science,* **124**, 194–199.

Pinaffi, F. L. V., É. S. Santos, M. G. Silva, M. Maturana, E. H. Madureira & L. A. Silva, 2015. Follicle and corpus luteum size and vascularity as predictors of fertility at the time of artificial insemination and embryo transfer in beef cattle. *Pesquisa Veterinária Brasileira,* **35**, 470–476.

Reynolds, L. P., A. T. Grazul-Bilska & D. A. Redmer, 2002. Angiogenesis in the female reproductive system: Pathological implications. *International Journal of Experimental Pathology*, **83**, 151–164.

Roche, J. F. & M. P. Boland, 1991. Turnover of dominant follicles in cattle of different reproductive states. *Theriogenology*, **35**, 81–90.

Roy, D., A. Bhattacharya & S. Luktuke, 1972. Estrous and ovarian activity of buffaloes in different months. *Indian Veterinary Journal,* **49**, 54–60.

Samir, H., M. M. Kandiel, A. M. Abo EL-Maaty, M. Sediqyar, K. Sasaki & G. Watanabe, 2019. Ovarian follicular changes and hemodynamics in Egyptian buffaloes under CIDR-PGF2α and Ovsynch-CIDR estrous synchronization treatments. *Journal of Reproduction and Development,* **65**, 451–457.

Satheshkumar, S., A. Sivakumar, S. Raja, P. Jayaganthan, V. Prabaharan & R. C. Rajasundaram, 2017. Color Doppler indices of ovarian artery in relation to ovarian activity in crossbred cattle. *Indian Journal of Animal Reproduction,* **38**, 614–625.

Siddiqui, M. A., M. Almamun & O. J. Ginther, 2009a. Blood flow in the wall of the preovulatory follicle and its relationship to pregnancy establishment in heifers. *Animal Reproduction Science,* **113**, 287–292.

Siddiqui, M. A. R., E. L. Gastal, M. O. Gastal, M. Almamun, M. A. Beg & O. J. Ginther, 2009b. Relationship of vascular perfusion of the wall of the preovulatory follicle to in vitro fertilisation and embryo development in heifers. *Reproduction*, **137**, 689–697.

Siddiqui, M. A., J. C. Ferreira, E. L. Gastal, M. A. Beg, D. A. Cooper & O. J. Ginther, 2010. Temporal relationships of the LH surge and ovulation to echotexture and power Doppler signals of blood flow in the wall of the preovulatory follicle in heifers. *Reproduction Fertility Development,* **22**, 1110–1117.

Silva, L. A., E. L. Gastal, M. O. Gastal, M. A. Beg & O. J. Ginther, 2006. Relationship between vascularity of the preovulatory follicle and establishment of pregnancy in mares. *Animal Reproduction,* **3**, 339–346.

Singh, G., R. K. Chandolia, R. Dutt, A. Saini & R. K. Malik. 2018. Characteristics of middle uterine artery and umbilical blood flow in pregnant Murrah buffalo. *Indian Journal of Animal Reproduction,* **39**, 11–14.

SPSS, 2016. IBM SPSS Inc Chicago ILUSA. Copyright© for Windows version 20.0 IBM SPSS.

Varughese, E. E., P. S. Brar & S. S. Dhindsa, 2013. Uterine blood flow during various stages of pregnancy in dairy buffaloes using transrectal Doppler ultrasonography. *Animal Reproduction Science,* **140**, 34.

Viana, J. H. M., E. K. N. Arashiro, L. G. B. Siqueira, A. M. Ghetti, V. S. Areas & C. R. B. Guimarães, 2013. Doppler ultrasonography as a tool for ovarian management. *Animal Reproduction,* **10**, 215–222.

Paper received 20.04.2021; accepted for publication 10.08.2021

Correspondence:

K.H. El-Shahat
Theriogenology Department,
Faculty of Veterinary Medicine,
Cairo University, Giza square, 12211
mobile: 00201064688386
e-mail: khattia90@gmail.com